Received: 29 March 2019 | Revised: 29 July 2019 | Accepted: 13 August 2019

DOI: 10.1111/bcp.14102

ORIGINAL ARTICLE

CD4+ count-dependent concentration–effect relationship of rituximab in rheumatoid arthritis

Amina Bensalem[1] | Denis Mulleman[1,2] | Gilles Thibault[1,3,4] | Nicolas Azzopardi[1,4] | Philippe Goupille[1,2] | Gilles Paintaud[1,5] | David Ternant[1,5]

[1]EA 7501 GICC, Université de Tours, Tours, France

[2]Department of Rheumatology, CHRU de Tours, Tours, France

[3]Laboratory of Immunology, CHRU de Tours, Tours, France

[4]ERL 7001, CNRS, Tours, France

[5]Department of Medical Pharmacology, CHRU de Tours, Tours, France

Correspondence
David Ternant, Université de Tours. EA 7501 GICC, Tours, France.
Email: david.ternant@univ-tours.fr

Aims: Rituximab is approved in rheumatoid arthritis (RA). A substantial decrease in CD4+ count was observed in responders after a single cycle of treatment. This study aimed to describe and quantifying the influence of CD4+ count depletion on the concentration–response relationship of rituximab in RA patients.

Methods: In this retrospective monocentric observational study, 52 patients were assessed. Repeated measurements of rituximab concentrations (pharmacokinetics), CD4+ counts (biomarker) and disease activity score in 28 joints (DAS28, clinical response) were made. Rituximab pharmacokinetics was described using a 2-compartment model, and CD4+ cell counts and DAS28 measurements were described using indirect turnover and direct Emax pharmacokinetic–pharmacodynamic models, respectively. Delay between rituximab concentrations and responses was accounted for by including biophase compartments.

Results: Elimination half-life of rituximab was 18 days. The pharmacokinetic–pharmacodynamic model showed that DAS28 response to rituximab was partly associated with CD4+ cell depletion. At 6 months, a deeper DAS28 decrease was observed in patients when CD4+ cell count is decreased: median [interquartile range] of DAS28 was 3.7 [2.9–4.4] and 4.5 [3.7–5.3] in patients with and without CD4+ decrease, respectively.

Conclusions: This is the first study to quantify the relationship between rituximab concentrations, CD4+ count and DAS28 in RA patients. This model showed that approximately 75% of patients had CD4+ count decrease, and that the clinical improvement is 2-fold higher in patients with CD4+ cells decrease than in others.

KEYWORDS

pharmacodynamics, pharmacokinetics, rheumatoid arthritis, rituximab, T-lymphocytes

1 | INTRODUCTION

Rituximab is a chimeric immunoglobulin G (IgG)1 monoclonal antibody that targets CD20, a protein present at the surface of most normal and neoplastic B lymphocytes.[1] It is approved as a second-line treatment in rheumatoid arthritis (RA) patients[2] but approximately half of patients do not respond to this treatment.[3] There is a large interindividual variability in rituximab pharmacokinetics (PK) in RA patients.[4,5] However, no relationship was reported between rituximab serum concentrations and clinical efficacy.

Several studies have shown associations between biomarkers related to B cells and clinical response to rituximab in RA. These biomarkers include rheumatoid factor (RF) presence, anti-citrullinated protein antibody (ACPA) levels, B-cell subset counts—notably memory

B cells—and levels of chemokines produced by B cells.[6-13] However, the quantitative relationship between depletion of peripheral blood B cells and clinical response is unclear. Indeed, rituximab induces a rapid, deep, and durable depletion of B cells in all RA patients, independently from their clinical response.[14-16] Moreover, B cell recovery is variable and does not seem to be associated with the duration of clinical response.[16]

T-cells have been known for decades to be involved in RA pathogenesis,[17-19] with a CD4+/CD8+ blood ratio higher than in healthy subjects.[20] Recent studies reported a substantial decrease of T cells, mainly CD4+ cells, after rituximab treatment in most RA patients: the more the CD4+ cells depletion, the better the clinical response.[14,15,21] In our previous study on this cohort, we showed that 1-half of patients had a 37% decrease of CD4+ counts in average 12 weeks after first rituximab course.[14] The rituximab-induced decrease of CD4+ cells might be explained by a decrease in antigen presentation and in co-stimulation associated with cooperation with B cells,[1,22-24] although, the precise mechanism is still unclear.

Although an association between CD4+ cells decrease induced by rituximab and clinical improvement of RA patients was confirmed,[14,15,21] a quantitative relationship between rituximab concentrations, cellular changes and clinical improvement has never been reported in the literature. Therefore, this work aimed at describing the dose–concentration–response relationship of rituximab in RA patients, using CD4+ counts and clinical response as endpoints.

What is already known about this subject

- Rituximab is effective in rheumatoid arthritis but its dose–response relationship is highly variable between patients.
- Rituximab serum concentrations may explain differences in response between patients.
- Clinical response of rheumatoid arthritis patients to rituximab was reported to be associated with depletion of T cells, especially CD4+ cells.

What this study adds

- The relationships between rituximab concentrations and CD4+ counts, and disease activity, were described using indirect and direct Emax models, respectively.
- Results suggest that rituximab serum concentrations partly explain clinical response.
- CD4+ depletion explains half of the clinical response to rituximab: decrease in disease activity (DAS28) in patients with CD4+ decrease is twice that of patients without CD4+ decrease.

2 | METHODS

2.1 | Study design

The present study is an analysis of the data of a retrospective cohort of 70 RA patients in whom rituximab was started between January 2007 and September 2012 in the rheumatology department of Tours University Hospital. Patients fulfilled American College of Rheumatology (ACR) criteria and received at least 1 rituximab course. Follow-up visits for clinical evaluation were scheduled at 3, 6 and around 10 months after the second infusion, as previously described.[14] This study was performed in accordance with the guidelines of the French Society of Rheumatology.[25] As individual results for serum rituximab concentrations were sent to the prescriber within the framework of a routine therapeutic drug monitoring service and discussed during clinic-biological rounds, ethical approval and informed consent were not sought.[5] To ensure accuracy of estimated PK and PK–pharmacodynamic (PD) parameters, patients were assessed in the present study if they had at least 3 non-0 measurements of rituximab concentrations and CD4+ counts; and only the first cycle data were used. The characteristics of assessed and nonassessed patients of the cohort were compared. The continuous and categorical variables of the 2 groups were compared using Mann–Whitney test and Fisher's exact test, respectively. These tests were 2-tailed, with $\alpha = 0.05$. These analyses were performed using R studio software.[26]

2.2 | Data

2.2.1 | Rituximab concentrations

Blood samples for rituximab serum concentration measurements were collected before, 2 hours after the end of each rituximab infusion and at each follow-up visit, and finally before the second rituximab cycle if any. Rituximab concentrations were determined by a validated ELISA derived from Blasco *et al.*[27] The limit of detection was 0.061 mg/L and the lower and upper limits of quantification were 0.20 and 9.0 mg/L, respectively.[5] To provide unbiased PK parameter estimates, the concentrations between 0 and 0.061 mg/L were censored.

2.2.2 | Biological data

Erythrocyte sedimentation rate, C-reactive protein, albumin and ACPA were measured at baseline and presence or absence of RF was assessed. Counts of CD4+ and CD19+ were performed prior to each rituximab infusion and at each follow-up visit using flow cytometry, as previously described and without additional sampling.[14] Pretherapeutic serum concentrations of IgG were measured (g/L) by nephelometry (BN TM II nephelometer, Siemens Healthcare Ltd, UK). Levels of serum albumin and C-reactive protein, and erythrocyte sedimentation rate were measured in the Biochemistry Laboratory of the University Hospital Center of Tours, whereas RF and ACPA concentration, and CD4+ and CD19+ counts and serum IgG concentrations were measured in the Immunology Laboratory, University Hospital of Tours, prior to each rituximab infusion.

2.2.3 | Clinical endpoints

Disease activity was assessed using DAS28 prior to each rituximab infusion and at each follow up visit.[28] DAS28 is considered as low if DAS28 ≤ 3.2[29] or patients in remission if DAS28 < 2.6. A change of 1.2 (twice the measurement error) in DAS28 is considered as a meaningful change.[30]

2.3 | PK and PK-PD analysis

2.3.1 | Software

Rituximab concentrations and response data were analysed using nonlinear mixed-effects modelling with Monolix suite 2018R1 (Lixoft, Orsay, France). To ensure the best convergence of the stochastic approximation expectation–maximization (SAEM) algorithm, large numbers of iterations were performed (K1 = 1000 and K2 = 300, where K1 and K2 are the *iteration kernels* 1 and 2 in Monolix). Two Markov chains were used. The Fisher information matrix and likelihood were computed using stochastic approximation and importance sampling, respectively. All PK and PK-PD models were run simultaneously.

2.3.2 | Structural model design

Rituximab concentrations were described using a 2-compartment model with microconstant parameterization, as previously described.[5]

The relationship between rituximab concentration, CD4+ count and DAS28 was described through 3 steps: description of (i) concentration–CD4+ count relationship; (ii) concentration–clinical response relationship; and (iii) the relationship between concentration, CD4+ count and clinical response.

Concentration-CD4+ count relationship

Since rituximab targets CD20+ cells and only 3% of T lymphocytes express CD20 on their membrane,[31] CD4+ depletion should not reflect its direct action on CD4+ cells, although a rituximab-mediated CD4+ cell elimination cannot be excluded.[32,33] Therefore, indirect models with either inhibition of CD4+ input or stimulation of CD4+ output were tested.

$$\frac{dL}{dt} = k_{in}.\left(1 - \frac{C}{CL_{50} + C}\right) - k_{out}.L \quad L_0 = \frac{k_{in}}{k_{out}} \qquad \text{(Model1)}$$

$$\frac{dL}{dt} = k_{in} - k_{out}.L.\left(1 + \frac{L_{max}.C}{CL_{50} + C}\right) \qquad \text{(Model1)}$$

where L and L_0 are CD4+ counts and CD4+ counts at baseline, k_{in} and k_{out} are zero-order input rate and first-order output rate of CD4+ counts, respectively, C is rituximab concentration and CL_{50} is rituximab concentration leading to a 50% decrease of CD4+ counts.

In addition, a biophase compartment was tested as follows:

$$\frac{dC_{eL}}{dt} = k_{eL}.(C_p - C_{eL}) \qquad \text{(Biophase1)}$$

where k_{eL} is first order biophase rate constant and C_p and C_{eL} are central (plasma) and biophase rituximab concentration, respectively. In model 1, C is either concentration in the central compartment (C_p) in absence of biophase compartment, or in biophase compartment (C_{eL}).

Concentration–clinical response relationship

The relationship between rituximab concentrations and DAS28 was described with a direct inhibitory Emax model. Neither the use of Hill term nor cell life span models improved model fitting (data not shown). Direct inhibitory Emax model as follows:

$$DAS = DAS_0.\left(1 - \frac{C}{CDAS_{50} + C}\right) \qquad \text{(Model2)}$$

where DAS and DAS_0 are DAS28 and DAS28 at baseline, C is rituximab concentration and $CDAS_{50}$ is rituximab concentration leading to a 50% decrease of DAS28.

In addition, a biophase compartment was tested as follows:

$$\frac{dC_{eDAS}}{dt} = k_{eDAS}.(C_p - C_{eDAS}) \qquad \text{(Biophase2)}$$

where C_{eDAS} is biophase rituximab concentration, and k_{eDAS} is first order biophase rate constant. In model 2, C is either in the central compartment (C_p) in absence of biophase compartment, or in biophase compartment (C_{eDAS}). The parameter k_{eDAS} was poorly estimable. This has been overcome by assuming that k_{eL} and k_{eDAS} were proportional. Early attempts showed that $k_{eDAS} = \frac{k_{eL}}{10}$.

Concentration–CD4+ count–clinical response relationship

The objective of this step was to show that rituximab-induced CD4+ depletion contributes, at least in part, to the clinical response. For this, the model describing concentration–CD4+ count relationship was run simultaneously with Emax models describing variations of DAS28 as follows:

1. *Clinical response depends only on rituximab concentrations*. DAS28 variations depend only on rituximab concentrations, as previously described using model (2). This model is used as a reference of noninfluence of CD4 count on clinical response.
2. *Clinical response depends on CD4+ counts*. Evolution of DAS28 depends only on CD4+ depletion, described as follows:

$$DAS = DAS_0.\left(1 + \left(LDAS_{50}.\frac{k_{out}}{k_{in}}\right)\right).\left(\frac{L}{LDAS_{50} + L}\right) \qquad \text{(Model3)}$$

where $LDAS_{50}$ is the CD4+ counts leading to a 50% decrease of DAS28. The relationship between CD4+ counts and DAS28 is based on a stimulatory direct model, because of the positive correlation of these 2 variables. The scaling factor involving $LDAS_{50}$, k_{in} and k_{out}

allows a DAS_0 value independent from CD4+ counts depletion, as demonstrated in appendix. This model assumes that DAS28 variations are only due to CD4+ count variations.

3. *Clinical response depends on both CD4+ counts and rituximab concentrations*. Evolution of DAS28 depends on both rituximab-induced CD4+ depletion and rituximab concentrations, described as follows:

$$DAS = DAS_0 \cdot \left(1 + \left(LDAS_{50} \cdot \frac{k_{out}}{k_{in}}\right)\right) \cdot \left(\frac{L}{LDAS_{50} + L}\right) \cdot \left(1 - \left(\frac{C}{CDAS_{50} + C}\right)\right) \quad \text{(Model4)}$$

In some patients, $LDAS_{50}$ values were very high, leading to a bimodal interindividual distribution. Therefore, distribution of LDAS50 was hardly estimable and between-subject model mixture (BSMM) was tested for each assumed concentration–CD4+ count-clinical response relationships.[34] BSMM models assume subpopulations of individuals which differ by their concentration–CD4+ count relationship. The alternative model described CD4+ counts was defined as follows:

$$\frac{dL}{dt} = k_{in} - k_{out} \cdot L \quad \text{(Model5)}$$

which corresponds to no influence of rituximab on CD4+ count. Each subject is assumed to belong to 1 of these subpopulations. The status of each patient is considered as unknown *a priori*. The BSMM model relies on the estimation of the probability (*P*) for patients to belong to the subpopulation with CD4+ depletion, or without depletion (1 – *P*). For a given patient, the group is estimated as the group of highest conditional probability (given data and model parameters).

2.3.3 | Interindividual and residual models

The interindividual variability of structural parameters was described using exponential model. Interindividual variances were fixed to 0 when residual error of random effects and/or their shrinkages were high.[35] Interindividual variability $LDAS_{50}$ and k_{eL} were poorly estimable and were therefore fixed to 0. Additive, proportional and mixed additive-proportional residual error models were tested.

2.3.4 | Influence of covariates

The categorical covariates (CAT) were sex, past anti-tumour necrosis factor-α use, corticosteroid and methotrexate cotreatment. The influence of categorical covariate on a given parameter was implemented as: $\ln(\theta_{TV}) = \ln(\theta_{CAT=0}) + \beta_{CAT=1}$, where $\theta_{CAT=0}$ is the value of θ for the reference category, and $\beta_{CAT=1}$ is a parameter modifying the typical value for the other category. Continuous covariates (COV) were age, body surface area (BSA), baseline IgG albumin serum concentrations and CD19+ counts. All the continuous covariates were centred on their median and implemented using a power model as follows: $\theta_i = \theta_0 \cdot \left(\frac{COV}{med(COV)}\right)^{\beta_{COV}}$, where θ_0 is the θ value for a median subject, β_{COV} quantifies the influence of COV on θ and med(COV) is the median value of COV.

2.3.5 | Model comparison and covariate selection

Structural models were compared using Akaike information criterion (AIC), which combines the objective function value (OFV) and the number of parameters to be estimated. For each relationship, the model with the lowest AIC was chosen. The OFV of the interindividual, residual and covariate models were compared using likelihood ratio test (LRT) since the difference in OFV (ΔOFV) between 2 models is assumed to follow a χ^2 distribution.

The influence of potential covariates on structural parameters was assessed in 2 steps: (i) a univariate step in which the influence of each covariate on structural parameters associated with interindividual variability was tested separately from the others. Covariates showing a significant influence ($\alpha < 0.05$) were kept for the (ii) multivariate step, in which a forward–backward stepwise selection process was made. In the forward stepwise, covariates showing a significant association with pharmacokinetic parameters ($\alpha < 0.05$) were added individually to the base model. In the backward stepwise, covariates which removal resulted in a statistically significant re-increase ($\alpha < 0.01$) were kept in the final model.

2.3.6 | Model goodness of fit and evaluation

All models were evaluated graphically using goodness-of-fit diagnostic plots: observed concentrations, CD4 counts, DAS28 *vs* population and individual predicted concentrations, CD4 counts, DAS28, respectively; individual and population weighted residuals distribution of concentrations, CD4 counts, DAS28 *vs* population predicted concentrations, CD4 counts, DAS28, respectively. Visual predictive checks and normalized prediction distribution errors were also performed by simulating 1000 replicates using the population model parameters.

2.4 | Simulations

To show the contribution of CD4+ depletion on clinical response, structural and interindividual parameters estimated using the final model describing concentration–CD4+ count–clinical response relationship were used to simulate DAS28 *vs* time profiles for different values of CL_{50} (5, 15, 50, 75 mg/l). As a reference, DAS28 was also simulated for no depletion of CD4+ counts. These simulations allowed to estimate the proportion of patients with low disease activity (DAS28 < 3.2) and in remission (DAS28 < 2.6).

To assess the contribution of covariates influencing rituximab pharmacokinetics and/or PK-PD on clinical response, we simulated typical profiles for the reference typical subject, lowest/highest continuous covariate values and each category of discrete covariate.

3 | RESULTS

Out of 70 patients of the retrospective cohort, 52 were assessable by PK-PD analysis (Table 1). Included and excluded patients differed only by methotrexate cotreatment, (respectively, 52 *vs* 22%, Table 1).

3.1 | PK and PK-PD modelling

A total of 270 blood samples, 254 CD4+ counts and 229 DAS28 measurements were available; 13.7% blood samples showed a rituximab concentration below LLOQ and were therefore censored.

PK model. Using a structural 2-compartment model, intercompartmental transfer rate constants (k_{12} and k_{21}) had high relative standard errors and their estimated values were close (approximately 0.1/d) and highly correlated (r^2 = 0.89). Therefore, a common value for k_{12} and k_{21} ($k_{12} = k_{21} = k_T$) was included in the model. Typical value of k_T was estimated with good accuracy and its interindividual variance (ω^2 k_T) was not estimable and was therefore fixed to 0. This model was better than a structural 1-compartment model (ΔAIC = 205.61). It described observed rituximab concentrations satisfactorily and PK parameters were estimated with good accuracy (Table 3).

Concentration–CD4+ count relationship. The indirect model with an inhibition of CD4 input (Model 1) had lower AIC with than without biophase compartment (ΔAIC = 59.7) and was therefore chosen (Table 2). Early attempts with the concentration–CD4 relationship model identified a high collinearity between k_{out} and k_{in}. We therefore fixed k_{out} to the value observed in these attempts, i.e. 0.014/d. This value was shown to be relevant using sensitivity analysis (lowest AIC among tested values) and corresponded to a CD4+ elimination half-life of 50 days ($t_{1/2} = \frac{\ln(2)}{k_{out}}$).

Concentration–clinical response relationship. The direct inhibitory Emax model (Model 2) with a biophase compartment had lower AIC compared to the model without biophase compartment (ΔAIC = 74.15), and was therefore chosen (Table 2). Fixing $k_{eDAS} = \frac{k_{eL}}{10}$ was shown to be relevant using sensitivity analysis (lowest AIC among tested values) and led to decrease AIC compared to no fixed ratio (ΔAIC = 3.69).

Concentration–CD4+ count–clinical response relationship. The interindividual variance was hardly estimable for models with relationship between CD4+ counts and DAS28. This has been overcome using the mixture of models (BSMM). Indeed, lower AIC were obtained for

TABLE 1 Baseline characteristics of patients included in the study and those excluded

Characteristics	Included patients	Excluded patients	*P*-value
Number	52	18	
Women, *n* (%)	43 (82.69)	15 (83.33)	>.999
Age, median (range), y	60 (36–85)	63.5 (45–82)	.19
BSA, median (range), m^2	1.77 (1.33–2.3)	1.74 (1.35–1.94)	.15
Weight (kg)	69.5 (40–108)	65 (42–82)	.12
Initial DAS28, median (range)	5.41 (3.32–8.35)	4.58 (2.08–7.47)	.27
ΔDAS28, median (range)	1.4 (–0.37–5.4)	0.67 (–2.6–4.0)	.12
CRP, median (range), mg/L	17.9 (1.4–148.6)	15.65 (1–120.6)	.35
Albumin, median (range), g/L	35.9 (27.9–44.6)	35.4 (28.7–43.1)	.80
Rheumatoid factor positive, *n* (%)	34 (65)	13 (72)	.77
ACPA positive, *n* (%)	45 (87)	16 (89)	>.999
Past anti-TNF use, *n* (%)	42 (81)	14 (78)	.74
Corticosteroids, *n* (%)	42 (81)	14 (78)	.74
Methotrexate, *n* (%)	27 (52)	4 (23)	**.05**
Serum IgG concentration, median (range), g/L	10.2 (5.01–25.1)	9.86 (5.87–17.5)	.47
Serum IgA concentration, median (range), g/L	2.78 (0.86–6.06)	2.39 (0.23–6.26)	.28
Serum IgM concentration, median (range), g/L	1.27 (0.42–3.66)	1.46 (0.3–5.64)	.44
CD19 count, median (range), /μL	202.5 (43–706)	230.5 (25–578)	.77
CD4 count, median (range), /μL	1238 (233–2882)	1054 (445–2330)	.26
CD3 count, median (range), /μL	1749 (323–3378)	1524 (675–2757)	.42
CD8 count, median (range), /μL	479 (139–1114)	419.5 (120–1123)	.28
NK CD3-CD56+, median (range), /μL	131 (13–654)	108.5 (33–345)	.31

Included patients in the pharmacokinetic–pharmacodynamic analysis were compared with excluded patients.
P values were obtained with the Mann–Whitney test (continuous variables) or Fisher's exact test (categorical variables).
BSA, body surface area; DAS28, disease activity score in 28 joints; ΔDAS28, the decrease of DAS28 at 6 months; CRP, C-reactive protein concentration; ACPA, anti-citrullinated protein antibody; IgG, immunoglobulin; TNF, tumour necrosis factor-α; NK, natural killer cells.

TABLE 2 Comparison of tested pharmacokinetic–pharmacodynamic (PK-PD) models

Relationships	PK-PD models		–2LL	AIC
RTX concentration–CD4+ counts	Indirect inhibition input		5774.11	5798.11
	Indirect inhibition input + biophase		**5710.41**	**5738.41**
	Indirect stimulation output		5738.94	5762.94
	Indirect stimulation output + biophase		5738.17	5766.17
	Cell life span		5740.24	5766.24
RTX concentration–clinical response	Direct		2764.98	2788.98
	Direct + biophase		**2688.83**	**2714.83**
RTX concentration–CD4-clinical response	No-BSMM	No lymphocyte-response link	6434.10	6470.10
		Full lymphocyte-response link	6480.09	6514.09
		Partial lymphocyte-response link	6436.99	6474.99
	BSMM	No lymphocyte-response link	6431.28	6469.28
		Full lymphocyte-response link	6424.63	6460.63
		Partial lymphocyte-response link	**6414.90**	**6454.90**

–2LL, –2 log-likelihood; AIC, Akaike information criterion; BSMM, between-subject model mixture; RTX, rituximab.

models with the use of BSMM (ΔAIC of 53.46 and 20.09 for models 3 and 4, respectively, Table 2). Model 4 (clinical response depending on both CD4+ counts and rituximab concentration) had lower AIC compared to model 3 (clinical response depending on CD4+ count) and model with clinical response depending on rituximab concentrations (ΔAIC = of 5.73 and 14.38, respectively, Table 2). The structural model 4 and BSMM was therefore chosen (Figure 1). The proportion of patients with CD4+ depletion estimated by BSMM modelling is 0.75. Thus, 1/4 of patients was susceptible to present no significant lymphocyte depletion, corresponding to an infinite value of CL_{50}.

Best error models were mixed additive–proportional, proportional and additive for rituximab concentrations, CD4+ counts and DAS28, respectively. Structural, interindividual and residual parameters were estimated with good accuracy (Table 3). Plots of predicted *vs* observed PK and PK-PD responses, individual-weighted residuals, population-weighted residuals, visual predictive checks and normalized prediction distribution errors showed no obvious model misspecification (Figure 2). All diagnostic plots were obtained from the final model.

3.2 | Influence of covariates

During univariate analysis, sex was found to influence central volume of distribution (V_c) of rituximab, and both serum IgG concentrations and BSA were found to influence k_{10}. No significant association between CD4+ counts and PK parameters was detected, as well as no significant influence of tested covariates on PK-PD parameters was found. In the multivariate analysis, V_c was found to be higher in male than in female patients (LRT = 8.71) and k_{10} increased with serum IgG concentrations (LRT = 28.62), as well as with BSA (LRT = 7.89).

3.3 | Simulations

DAS28–time profiles showed deeper nadir for decreasing CL_{50} values (Figure 4). At 6 months, a greater DAS28 decrease was observed in patients when CD4+ cell count is decreased: predicted median [interquartile range] of DAS28 was 3.7 [2.9–4.4] and 4.5 [3.7–5.2] in patients with and without CD4+ decrease, respectively (Figure 3b). This corresponds to a DAS28 decrease (ΔDAS28) was observed in patients with CD4+ cell count decrease as compared to others: predicted median [interquartile range] ΔDAS28 being 1.5 [0.8–2.3] and 0.7 [0–1.5], respectively. Estimated proportion of patients with low disease activity (DAS28 ≤ 3.2) and in remission (DAS28 < 2.6) among patients with CD4+ counts decrease (32.3% and 20.7%, respectively) were higher than in patients without CD4+ counts decrease (14.3% and 6.9%, respectively).

Regarding the contribution of covariates influencing rituximab pharmacokinetics, we simulated reference subject (female sex, median

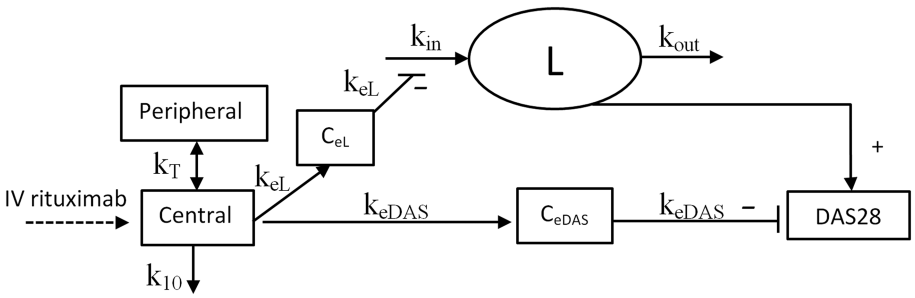

FIGURE 1 Schematic of the final multiresponse pharmacokinetic–pharmacodynamic model. IV, intravenous; T, CD4+ cells; k_{10}, first-order elimination rate constant; k_T, first-order transfer rate constant; k_{in}, zero-order production rate constant; k_{out}, first-order loss rate constant; C_{eL} and C_{eDAS}, concentrations of rituximab in biophase linked lymphocyte and clinical response respectively; k_{eL} and k_{eDAS}, first-order biophase rate constants

TABLE 3 Pharmacokinetic–pharmacodynamic parameter estimates

Parameter (unit)	Estimate	RSE (%)	*P* value
Fixed effects			
V_c (L)	3.9	7	
Sex on V_c	0.48	36	.0057
k_{10} (/d)	0.093	4	
IgG on k_{10}	0.78	16	8.5×10^{-10}
BSA on k_{10}	0.85	34	.0032
k_T (/d)	0.11	11	
k_{eL} (/d)	0.0099	14	
k_{in} (μL/d)	17.2	7	
k_{out} (/d)	0.014	-	
CL_{50} (mg/L)	16.9	27	
Das_0	5.2	3	
$LDAS_{50}$ (μL^{-3})	269	33	
$CDAS_{50}$ (mg/L)	35.7	36	
P	0.75	12	
Interindividual and residual variability			
ω_{Vc} (%)	44.9	11	
ω_{k10} (%)	23	13	
ω_{kin} (%)	45.9	12	
ω_{CL50} (%)	108	20	
ω_{DAS_0} (%)	19.9	13	
ω_{CDAS50} (%)	134	20	
σ_{add1} (mg/L)	0.15	16	
σ_{prop1} (%)	24.2	7	
σ_{prop2} (%)	25	6	
σ_{add}	0.819	6	

BSA, body surface area; IgG, immunoglobulin G serum concentration; V_c, central distribution volume; k_{10}, first-order elimination rate; k_T, first-order transfer rate between the central and the peripheral compartment; k_{eL}, first-order biophase rate constant; k_{in}, zero order input rate of CD4+ counts; k_{out}, first order output rate of CD4+ counts; CL_{50} half maximal effective rituximab concentration leading to a 50% decrease of CD4+ counts; $CDAS_{50}$, half maximal effective rituximab concentration leading to a 50% decrease of DAS28; $LDAS_{50}$, half maximal effective CD4+ counts leading to a 50% decrease of DAS28; DAS_0, DAS28 at baseline; *P*, the probability of patients with CD4+ counts decreasing in the population. There is no interpatient variability on *P*: all subjects have the same probability to be with or without CD4+ counts decrease in this study. We use a logit-normal distribution for *P* in order to constrain it to be between 0 and 1 without variability; RSE residual standard error [RSE = (standard error/estimate) × 100]; ω interindividual standard deviation; σ_{add1}; σ_{add} additive residual standard deviation for rituximab concentrations data and DAS28; respectively; $\sigma_{prop1;}$ σ_{prop2} proportional residual standard deviation for rituximab concentrations data and CD4+ counts data, respectively

BSA and IgG levels) and typical subjects with lowest/highest BSA and IgG levels, and for male sex. The difference in nadir DAS28 was 0.5 between female and male patients, as well between lowest and highest BSA values; whereas this difference between lowest and highest IgG levels was 1.3 in patients with CD4+ depletion and 0.7 in patients without CD4+ depletion.

4 | DISCUSSION

To our knowledge, this study is the first to quantify the dose–concentration–response relationship of rituximab in RA patients using PK-PD modelling. Our multiresponse model satisfactorily described rituximab concentrations and continuous pharmacodynamic data, i.e. CD4+ counts and DAS28. Volume of distribution (V_c) and elimination constant (k_{10}) are close to those previously reported.[4,5] No nonlinearity in elimination or time-variation of PK parameters was detected. As in our previous study on the same cohort, male sex, and higher body surface area and IgG serum levels were associated with lower rituximab concentrations.[5] The nonsignificant association of CD19 with PK parameters contrary to our previous study may be due to the fact that only the first rituximab course was considered here.

The concentration–response relationship of rituximab was highly variable among patients. The use of CD4+ count as a biomarker of rituximab effect is justified by its relationship with clinical response.[14,15,21] The use of an indirect model with inhibition of input to describe the concentration–CD4+ relationship is justified by a possible mechanism of rituximab-induced T cell decrease. As rituximab targets B cells, the decrease of CD4+ cells may be due to the lack of antigen presentation by B cells, and lack of co-stimulation as long as the levels of such cytokines and specific peptides of B cells were reduced.[22-24] Moreover, this indirect model was improved by the addition of a biophase compartment, which is compatible with: (i) the delay between rituximab concentrations and their effect on circulating CD4+ cells and (ii) the fact that rituximab is effective not only in blood, but also in other loci, as synovia.[36] Other modelling strategies based on cell lifespan models[37] were attempted, but did not lead to a better description of CD4+ data.

The direct inhibitory model allowed a satisfactory description of clinical response, assessed by DAS28. This model gave better results than an indirect model—notably because input and output rate constants were hardly identifiable—but was improved by the use of a biophase compartment.

A direct model was previously used to describe concentration–DAS28 relationship, in RA patients treated with adalimumab, but without biophase compartment.[38,39] The use of BSMM was motivated by the fact that interindividual distribution of the $LDAS_{50}$ CD4+ count was bimodal. This approach was superior to considering a residual disease activity associated with CD4+ count in presence of high rituximab concentrations (data not shown).

More than confirming that rituximab-induced depletion of CD4+ cell count contributes, at least in part, clinical improvement of RA patients,[14,15,21] our final model shows that, on average, decrease in DAS28 is doubled in patients with significant CD4+ cell depletion (ΔDAS28 of 1.5 *vs* 0.7).

The depletion of CD4+ cells, as well as clinical improvement independent from CD4 depletion, are highly variable, notably because of a

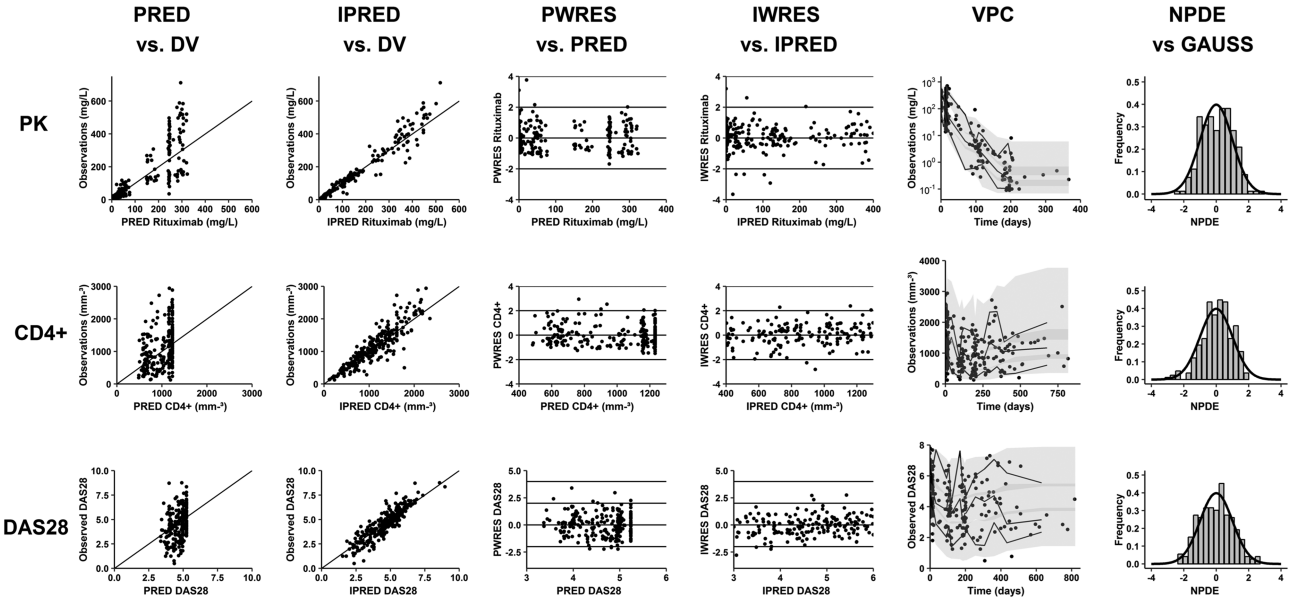

FIGURE 2 Diagnostic plots of the final pharmacokinetic (PK)–pharmacodynamic multiresponse (PK-CD4-DAS28) model. The plots show population model-predicted (PRED) and individual model-predicted (IPRED) *vs* observed data (DV); individual weighted residuals (IWRES) and population weighted residuals (PWRES) *vs* PRED; visual predictive checks (VPCs): circles are data, solid lines are low, median and high empirical percentiles of simulated data, and shaded areas are 10, 50 and 90% prediction intervals; distribution frequency of normalized prediction distribution errors (NPDE) *vs* Gaussian (gauss) law. Plots are for PK, CD4+ counts and DAS28 data from top to bottom

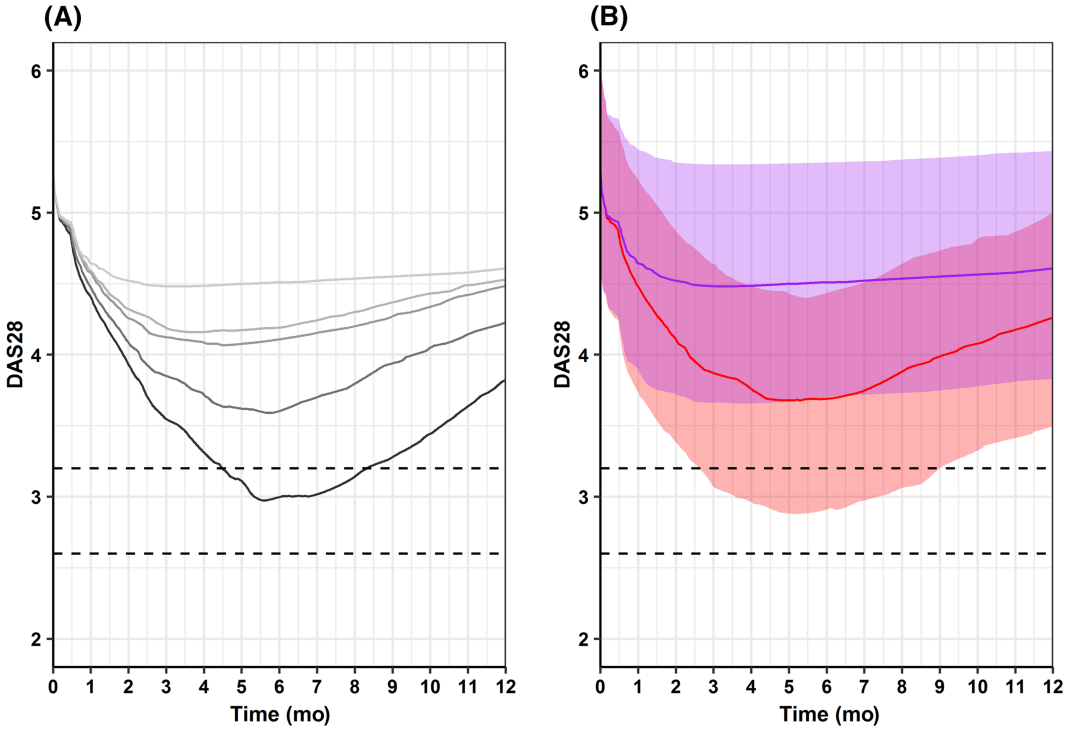

FIGURE 3 Simulations of DAS28–time profile using structural and interindividual parameters estimated from the final model describing concentration–CD4 +–DAS28 relationship. (A) simulations of DAS28–time profile for increasing value of CL_{50} 5, 15, 50, 75 mg/L, and for no lymphocyte depletion (increasingly with grey gradient colour). (B) simulations of DAS28–time profile in patients with (red line) and without (purple line) CD4+ cell decrease. The central curve are the median dynamics of DAS28 and the shadow are interquartile prediction intervals. The limits of the reference score in both A and B are represented as low DAS28 ≤ 3.2, and remission DAS28 < 2.6

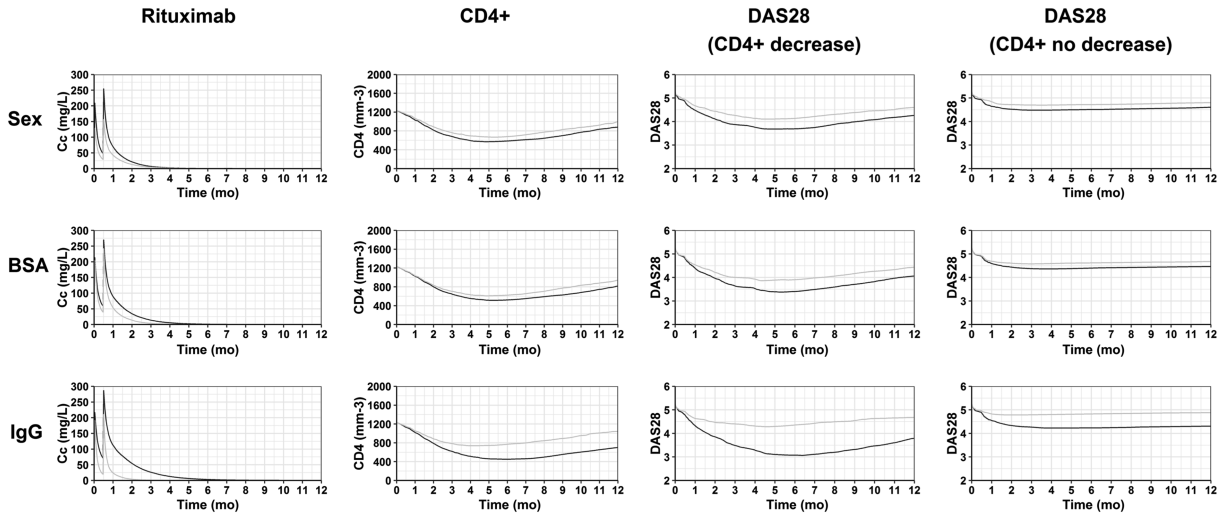

FIGURE 4 Simulations of, from left to right, rituximab concentrations, CD4+ counts, DAS28 in patients with CD4+ depletion and in patients without CD4+ depletion. From top to bottom, these simulations were made for males *vs* females, lowest *vs* highest BSA values and lowest *vs* highest IgG levels

large interindividual variability of concentration–CD4+ and concentration–DAS28 relationships. Despite this variability, simulations showed that covariates associated with rituximab pharmacokinetics, especially IgG levels, substantially altered the concentration–effect relationship: male sex, and increasing BSA and/or IgG levels being associated with substantial decrease of clinical response. Taken together, these results suggest that interindividual variations in rituximab concentrations may explain a notable part of the interindividual variability in DAS28 response.

The description of this relationship was not improved by adding CD19+ cell counts as a level between rituximab concentrations and CD4+ cell count (supplemental data). This relationship was not significantly influenced by the use of methylprednisolone before each rituximab infusion: indeed, CD4+ counts between first and second rituximab infusions were not significantly decreased (Wilcoxon paired test, 49 pairs, $p = 0.5212$).

Our model has limitations. First, if a second pharmacokinetic compartment was identifiable, the estimation of PK parameters of the peripheral compartment (transfer rate constants or peripheral volume and intercompartmental clearance) was not possible, which led us to estimate a global intercompartmental transfer rate (k_T), which still led to a satisfactory description of concentration data.

Second, the CD4+ output rate constant (k_{out}) was hardly estimable and was therefore fixed at a value obtained in early attempts (0.014/d); this value was verified with analysis of sensitivity and allowed a satisfactory description of CD4+ count and DAS28 data. In addition, corresponding estimated CD4+ cell elimination half-life was 50 days ($t_{1/2} = \frac{\ln(2)}{k_{out}}$). In the literature, very different values of this half-life were reported (between 11 days and 8 years).[40-45] This may be due to differences between CD4+ count techniques between patients and between diseases.

Third, rate constants of concentration–CD4+ counts and of concentration–DAS28 could not be estimated independently, their ratio was fixed at a value obtained in early attempts ($k_{eDAS} = \frac{k_{eL}}{10}$). This ratio was verified with analysis of sensitivity and allowed satisfactory description of PK-PD data. These rate constants, as well as their ratio, are difficult to interpret because their respective compartment effects apply to markers described using different models, i.e. indirect and direct models for CD4+ counts and DAS28 measurements, respectively. Since the delay between concentration and CD4+ count variations is accounted by both indirect and biophase compartments, the ratio of $\frac{ke_{DAS}}{ke_L}$ should be understood as DAS28 variations slower than those of CD4+ counts, but <10 fold. Since this study is the first to quantify the role of CD4+ counts on the dose–concentration–effect relationship of rituximab in RA, this ratio cannot be compared with previous estimations, but may be considered as a basis for future studies.

Fourth, the biophase rate constant integrated in the concentration–DAS28 relationship (k_{eDAS}) was poorly estimable. The best strategy tested was to fix this value as being 1/10 of the biophase rate constant of concentration–CD4+ response relationship (k_{eL}). This ratio, obtained in early attempts, led to a satisfactory description of DAS28 data.

5 | CONCLUSION

This is the first study quantifying the relationship between rituximab concentrations, CD4+ count and DAS28 in RA patients. Although rituximab concentrations are poorly predictive of clinical response, our model showed a substantial influence of rituximab pharmacokinetics on clinical response, a significant decrease of CD4+ count is obtained in approximately 75% of patients and that the decrease of

disease activity is doubled in presence of depletion of CD4+ cells over that in absence.

ACKNOWLEDGEMENTS

The authors thank Anne-Claire Duveau, Celine Desvignes and Caroline Guerineau-Brochon for their technical assistance in measuring rituximab concentration and to Audrey Dabert, Claudine Prouin and Françoise Vosgien in measuring IgG concentration. We thank Drs Saloua Mammou, Isabelle Griffoul, Emilie Ducourau, Virginie Martaillé, Francine Lauféron, Julien Mélet, Mathilde Marot, Sarah Butin and Frédéric Médina for helping with clinical assessment. We are indebted to Nelly Jaccaz-Vallée, Sergine Gosset, Valérie Angebeau, Laetitia Cornec, Adeline Coutellier, Corinne Depont, Vanessa Fougeray, Valérie Fuseau, Pascale Guibout, Sophie Joncheray, Céline Letot, Isabelle Romier and Elodie Vigneron for blood sampling and their commitment to taking care of patients. Measurements of rituximab serum concentrations were carried out within the CePiBAc platform. CePiBAc is cofinanced by the European Union. Europe is committed to the region Centre with the European Regional Development Fund. This work was partly supported by the French Higher Education and Research ministry under the programme *Investissements d'avenir* Grant Agreement: LabEx MAbImprove ANR-10-LABX-53-01. The authors have participated in the Consortium *Monitoring of monoclonal Antibodies Group in Europe* (MAGE) for inflammatory diseases. The MAGE Consortium is supported by LE STUDIUM Loire Valley Institute for Advanced Studies (http://www.lestudium-ias.com/). D.M., G.P., D.T. and G.P. are currently participating in the European League Against Rheumatism (Eular) Therapeutic Drug Monitoring Study Group. https://www.eular.org/clinical_affairs_study_groups.cfm

COMPETING INTERESTS

During the last 36 months D.M. has given lectures and his institution received consultancy fees from Grifols, Novartis, and Pfizer; he attended international congresses at the invite of Janssen-Cilag; and his university received research grants from the Lions Club Tours Val de France. G.P. reports grants from Novartis, grants from Roche Pharma, grants from Sanofi-Genzyme, grants from Chugai, grants from Pfizer, outside the submitted work. P.G. reports personal fees and nonfinancial support from Abbvie, Amgen, Biogaran, BMS, Celgene, Janssen, Lilly, MSD, Pfizer, Sanofi-Genzyme and UCB, outside the submitted work. D.T. has given lectures to Sanofi, Amgen and Boehringer Ingelheim, outside the submitted work. A.B., G.T. and N.A. have nothing to disclose.

CONTRIBUTORS

A.B. analysed and interpreted the data, and wrote the manuscript. D.M. designed the study, acquired data, participated in data interpretation and reviewed the manuscript. G.T. reviewed the manuscript. N.A. participated in data analysis and reviewed the manuscript. G.P. reviewed the manuscript. P.G. reviewed the manuscript. D.T. designed the study, supervised and participated in the writing of the manuscript, and reviewed the manuscript.

As part of the routine therapeutic drug monitoring of rituximab, blood samples are drawn to measure rituximab trough concentrations and individual results are interpreted and sent to the prescriber and discussed during clinic-biological rounds. The authors confirm that the Principal Investigator for this paper is Denis Mulleman and that he had direct clinical responsibility for patients.

DATA AVAILABILITY STATEMENT

I, David Ternant, corresponding author of this study, confirm the data availability of the routine practice cohort regarding the present study.

ORCID

David Ternant https://orcid.org/0000-0003-4020-4545

REFERENCES

1. Reff ME, Carner K, Chambers KS, et al. Depletion of B cells in vivo by a chimeric mouse human monoclonal antibody to CD20. *Blood*. 1994;83(2):435-445.
2. Smolen JS, Landewe R, Bijlsma J, et al. EULAR recommendations for the management of rheumatoid arthritis with synthetic and biological disease-modifying antirheumatic drugs: 2016 update. *Ann Rheum Dis*. 2017;76(6):960-977. https://doi.org/10.1136/annrheumdis-2016-210715 published Online First: Epub Date
3. Smolen JS, Aletaha D, Koeller M, Weisman MH, Emery P. New therapies for treatment of rheumatoid arthritis. *Lancet*. 2007;370(9602):1861-1874. https://doi.org/10.1016/S0140-6736(07)60784-3 published Online First: Epub Date
4. Ng CM, Bruno R, Combs D, Davies B. Population pharmacokinetics of rituximab (anti-CD20 monoclonal antibody) in rheumatoid arthritis patients during a phase II clinical trial. *J Clin Pharmacol*. 2005;45(7):792-801. https://doi.org/10.1177/0091270005277075 published Online First: Epub Date
5. Lioger B, Edupuganti SR, Mulleman D, et al. Antigenic burden and serum IgG concentrations influence rituximab pharmacokinetics in rheumatoid arthritis patients. *Br J Clin Pharmacol*. 2017;83(8):1773-1781. https://doi.org/10.1111/bcp.13270 published Online First: Epub Date
6. Ruyssen-Witrand A, Rouanet S, Combe B, et al. Association between -871C>T promoter polymorphism in the B-cell activating factor gene and the response to rituximab in rheumatoid arthritis patients. *Rheumatology (Oxford)*. 2013;52(4):636-641. https://doi.org/10.1093/rheumatology/kes344 published Online First: Epub Date
7. Sellam J, Rouanet S, Hendel-Chavez H, et al. Blood memory B cells are disturbed and predict the response to rituximab in patients with rheumatoid arthritis. *Arthritis Rheum*. 2011;63(12):3692-3701. https://doi.org/10.1002/art.30599 published Online First: Epub Date
8. Sellam J, Rouanet S, Hendel-Chavez H, et al. CCL19, a B cell chemokine, is related to the decrease of blood memory B cells and predicts the clinical response to rituximab in patients with rheumatoid arthritis. *Arthritis Rheum*. 2013;65(9):2253-2261. https://doi.org/10.1002/art.38023 published Online First: Epub Date
9. Dass S, Rawstron AC, Vital EM, Henshaw K, McGonagle D, Emery P. Highly sensitive B cell analysis predicts response to rituximab therapy in rheumatoid arthritis. *Arthritis Rheum*. 2008;58(10):2993-2999. https://doi.org/10.1002/art.23902 published Online First: Epub Date

10. Roll P, Dorner T, Tony HP. Anti-CD20 therapy in patients with rheumatoid arthritis: predictors of response and B cell subset regeneration after repeated treatment. *Arthritis Rheum*. 2008;58(6):1566-1575. https://doi.org/10.1002/art.23473 published Online First: Epub Date
11. Isaacs JD, Cohen SB, Emery P, et al. Effect of baseline rheumatoid factor and anticitrullinated peptide antibody serotype on rituximab clinical response: a meta-analysis. *Ann Rheum Dis*. 2013;72(3):329-336. https://doi.org/10.1136/annrheumdis-2011-201117 published Online First: Epub Date
12. Lal P, Su Z, Holweg CT, et al. Inflammation and autoantibody markers identify rheumatoid arthritis patients with enhanced clinical benefit following rituximab treatment. *Arthritis Rheum*. 2011;63(12):3681-3691. https://doi.org/10.1002/art.30596 published Online First: Epub Date
13. Narvaez J, Diaz-Torne C, Ruiz JM, et al. Predictors of response to rituximab in patients with active rheumatoid arthritis and inadequate response to anti-TNF agents or traditional DMARDs. *Clin Exp Rheumatol*. 2011;29(6):991-997.
14. Melet J, Mulleman D, Goupille P, Ribourtout B, Watier H, Thibault G. Rituximab-induced T cell depletion in patients with rheumatoid arthritis: association with clinical response. *Arthritis Rheum*. 2013;65(11):2783-2790. https://doi.org/10.1002/art.38107 published Online First: Epub Date
15. Lavielle M, Mulleman D, Goupille P, et al. Repeated decrease of CD4 + T-cell counts in patients with rheumatoid arthritis over multiple cycles of rituximab treatment. *Arthritis Res Ther*. 2016;18(1):253. https://doi.org/10.1186/s13075-016-1152-5 published Online First: Epub Date
16. Breedveld F, Agarwal S, Yin M, et al. Rituximab pharmacokinetics in patients with rheumatoid arthritis: B-cell levels do not correlate with clinical response. *J Clin Pharmacol*. 2007;47(9):1119-1128. https://doi.org/10.1177/0091270007305297 published Online First: Epub Date
17. Schmidt D, Goronzy JJ, Weyand CM. CD4+ CD7- CD28- T cells are expanded in rheumatoid arthritis and are characterized by autoreactivity. *J Clin Invest*. 1996;97(9):2027-2037. https://doi.org/10.1172/JCI118638 published Online First: Epub Date
18. Goronzy JJ, Bartz-Bazzanella P, Hu W, Jendro MC, Walser-Kuntz DR, Weyand CM. Dominant clonotypes in the repertoire of peripheral CD4+ T cells in rheumatoid arthritis. *J Clin Invest*. 1994;94(5):2068-2076. https://doi.org/10.1172/JCI117561 published Online First: Epub Date
19. Gregersen PK, Silver J, Winchester RJ. The shared epitope hypothesis. An approach to understanding the molecular genetics of susceptibility to rheumatoid arthritis. *Arthritis Rheum*. 1987;30(11):1205-1213.
20. Hussein MR, Fathi NA, El-Din AM, et al. Alterations of the CD4(+), CD8 (+) T cell subsets, interleukins-1beta, IL-10, IL-17, tumor necrosis factor-alpha and soluble intercellular adhesion molecule-1 in rheumatoid arthritis and osteoarthritis: preliminary observations. *Pathol Oncol Res*. 2008;14(3):321-328. https://doi.org/10.1007/s12253-008-9016-1 published Online First: Epub Date
21. Piantoni S, Scarsi M, Tincani A, Airo P. Circulating CD4+ T-cell number decreases in rheumatoid patients with clinical response to rituximab. *Rheumatol Int*. 2015;35(9):1571-1573. https://doi.org/10.1007/s00296-015-3295-0 published Online First: Epub Date
22. Liossis SN, Sfikakis PP. Rituximab-induced B cell depletion in autoimmune diseases: potential effects on T cells. *Clin Immunol*. 2008;127(3):280-285. https://doi.org/10.1016/j.clim.2008.01.011 published Online First: Epub Date
23. Rudulier CD, Kroeger DR, Bretscher PA. Distinct roles of dendritic and B cells in the activation of naive CD4+ T cells. *Immunotherapy*. 2012;4(4):355-357. https://doi.org/10.2217/imt.12.17 published Online First: Epub Date
24. Takemura S, Klimiuk PA, Braun A, Goronzy JJ, Weyand CM. T cell activation in rheumatoid synovium is B cell dependent. *J Immunol*. 2001;167(8):4710-4718.
25. Pham T, Fautrel B, Gottenberg JE, et al. Rituximab (MabThera) therapy and safety management. Clinical tool guide. *Joint Bone Spine*. 2008;75(Suppl 1):S1-S99. https://doi.org/10.1016/S1297-319X(08)73620-0 published Online First: Epub Date
26. RStudio, Version 1.1.383. RStudio: Integrated Development for R. RStudio, Inc., Boston, MA. Secondary RStudio, Version 1.1.383. RStudio: Integrated Development for R. RStudio, Inc., Boston, MA. http://www.rstudio.com/.
27. Blasco H, Lalmanach G, Godat E, et al. Evaluation of a peptide ELISA for the detection of rituximab in serum. *J Immunol Methods*. 2007;325(1–2):127-139. https://doi.org/10.1016/j.jim.2007.06.011 published Online First: Epub Date
28. Prevoo ML, van 't Hof MA, Kuper HH, van Leeuwen MA, van de Putte LB, van Riel PL. Modified disease activity scores that include twenty-eight-joint counts. Development and validation in a prospective longitudinal study of patients with rheumatoid arthritis. *Arthritis Rheum*. 1995;38(1):44-48.
29. van Gestel AM, Haagsma CJ, van Riel PL. Validation of rheumatoid arthritis improvement criteria that include simplified joint counts. *Arthritis Rheum*. 1998;41(10):1845-1850. https://doi.org/10.1002/1529-0131(199810)41:10<1845::AID-ART17>3.0.CO;2-K published Online First: Epub Date
30. van Gestel AM, Prevoo ML, van 't Hof MA, van Rijswijk MH, van de Putte LB, van Riel PL. Development and validation of the European league against rheumatism response criteria for rheumatoid arthritis. Comparison with the preliminary American College of Rheumatology and the World Health Organization/international league against rheumatism criteria. *Arthritis Rheum*. 1996;39(1):34-40.
31. Leandro MJ, Cambridge G, Ehrenstein MR, Edwards JC. Reconstitution of peripheral blood B cells after depletion with rituximab in patients with rheumatoid arthritis. *Arthritis Rheum*. 2006;54(2):613-620. https://doi.org/10.1002/art.21617 published Online First: Epub Date
32. Mulleman D, Thibault G. Reply: to PMID 23918413. *Arthritis Rheumatol*. 2014;66(4):1054-1055. https://doi.org/10.1002/art.38346 published Online First: Epub Date
33. Eggleton P, Bremer E. Direct and indirect rituximab-induced T cell depletion: comment on the article by Melet et Al. *Arthritis Rheumatol*. 2014;66(4):1053. https://doi.org/10.1002/art.38347 published Online First: Epub Date
34. Monolix version 2016R1. Secondary Monolix version 2016R1. http://monolix2016.lixoft.com/single-page/.
35. Savic RM, Karlsson MO. Importance of shrinkage in empirical bayes estimates for diagnostics: problems and solutions. *AAPS j*. 2009;11(3):558-569. https://doi.org/10.1208/s12248-009-9133-0 published Online First: Epub Date
36. Boumans MJ, Thurlings RM, Gerlag DM, Vos K, Tak PP. Response to rituximab in patients with rheumatoid arthritis in different compartments of the immune system. *Arthritis Rheum*. 2011;63(11):3187-3194. https://doi.org/10.1002/art.30567 published Online First: Epub Date
37. Perez-Ruixo JJ, Kimko HC, Chow AT, Piotrovsky V, Krzyzanski W, Jusko WJ. Population cell life span models for effects of drugs following indirect mechanisms of action. *J Pharmacokinet Pharmacodyn*. 2005;32(5–6):767-793. https://doi.org/10.1007/s10928-005-0019-1 published Online First: Epub Date
38. Ternant D, Ducourau E, Fuzibet P, et al. Pharmacokinetics and concentration-effect relationship of adalimumab in rheumatoid arthritis. *Br J Clin Pharmacol*. 2015;79(2):286-297. https://doi.org/10.1111/bcp.12509 published Online First: Epub Date

39. Ducourau E, Ternant D, Lequerre T, et al. Towards an individualised target concentration of adalimumab in rheumatoid arthritis. *Ann Rheum Dis*. 2014;73(7):1428-1429. https://doi.org/10.1136/annrheumdis-2013-204971 published Online First: Epub Date
40. Ternant D, Buchler M, Thibault G, et al. Influence of FcgammaRIIIA genetic polymorphism on T-lymphocyte depletion induced by rabbit antithymocyte globulins in kidney transplant patients. *Pharmacogenet Genomics*. 2014;24(1):26-34. https://doi.org/10.1097/FPC.0000000000000017 published Online First: Epub Date
41. Hellerstein M, Hanley MB, Cesar D, et al. Directly measured kinetics of circulating T lymphocytes in normal and HIV-1-infected humans. *Nat Med*. 1999;5(1):83-89. https://doi.org/10.1038/4772 published Online First: Epub Date
42. De Boer RJ, Perelson AS. Quantifying T lymphocyte turnover. *J Theor Biol*. 2013;327:45-87. https://doi.org/10.1016/j.jtbi.2012.12.025 published Online First: Epub Date
43. Farber DL, Yudanin NA, Restifo NP. Human memory T cells: generation, compartmentalization and homeostasis. *Nat Rev Immunol*. 2014;14(1):24-35. https://doi.org/10.1038/nri3567 published Online First: Epub Date
44. Vukmanovic-Stejic M, Zhang Y, Cook JE, et al. Human CD4+ CD25hi Foxp3+ regulatory T cells are derived by rapid turnover of memory populations in vivo. *J Clin Invest*. 2006;116(9):2423-2433. https://doi.org/10.1172/JCI28941 published Online First: Epub Date
45. Stein DS, Drusano GL. Modeling of the change in CD4 lymphocyte counts in patients before and after administration of the human immunodeficiency virus protease inhibitor indinavir. *Antimicrob Agents Chemother*. 1997;41(2):449-453.

SUPPORTING INFORMATION

Additional supporting information may be found online in the Supporting Information section at the end of this article.

How to cite this article: Bensalem A, Mulleman D, Thibault G, et al. CD4+ count-dependent concentration–effect relationship of rituximab in rheumatoid arthritis. *Br J Clin Pharmacol*. 2019;85:2747–2758. https://doi.org/10.1111/bcp.14102

APPENDIX

$$DAS1 = DAS_0 . \left(\frac{L}{LDAS_{50} + L} \right) . \left(1 - \left(\frac{C}{CDAS_{50} + C} \right) \right) \quad (A.1)$$

$$DAS2 = DAS_0 . \left(1 - \left(\frac{C}{CDAS_{50} + C} \right) \right) \quad (A.2)$$

Where DAS1 (equation 1) and DAS2 (equation 2) describe DAS in patients with and without CD4+ count depletion, respectively. It can be easily remarked that initial DAS values (DAS_0) are different for the 2 groups. Therefore, we use the notation DAS'_0 for DAS1:

$$DAS1 = DAS'_0 . \left(\frac{L}{LDAS_{50} + L} \right) . \left(1 - \left(\frac{C}{CDAS_{50} + C} \right) \right) \quad (A.3)$$

Now let us calculate a scaling factor to obtain $DAS_0 = DAS'_0$:

At time = 0, DAS1 should be equal to DAS2, then:

$$DAS'_0 . \left(\frac{L}{LDAS_{50} + L} \right) = DAS_0$$

and

$$DAS'_0 = DAS_0 . \left(\frac{LDAS_{50} + L}{L} \right)$$

At $t = 0$, $L = \frac{k_{in}}{k_{out}}$, then

$$DAS'_0 = DAS_0 . \left(\frac{LDAS_{50} + \frac{k}{k_{out}}}{\frac{k_{in}}{k_{out}}} \right)$$

and

$$DAS'_0 = DAS_0 . \left(1 + \left(LDAS_{50} . \frac{k_{out}}{k_{in}} \right) \right) \quad (A.4)$$

Replacing DAS'_0 in E.3 by its expression given in E.4:

$$DAS1 = DAS_0 . \left(1 + \left(LDAS_{50} . \frac{k_{out}}{k_{in}} \right) \right) . \left(\frac{L}{LDAS_{50} + L} \right) . \left(1 - \left(\frac{C}{CDAS_{50} + C} \right) \right) \quad (Model4)$$

which is model 4.